

Enhanced collectivity in neutron-deficient Sn isotopes in energy functional based collective Hamiltonian

Z. P. Li^a, C. Y. Li^a, J. Xiang^a, J. M. Yao^{a,b}, J. Meng^{c,d,e}

^aSchool of Physical Science and Technology, Southwest University, Chongqing 400715, China

^bPhysique Nucléaire Théorique, Université Libre de Bruxelles, C.P. 229, B-1050 Bruxelles, Belgium

^cState Key Laboratory of Nuclear Physics and Technology, School of Physics, Peking University, Beijing 100871, China

^dSchool of Physics and Nuclear Energy Engineering, Beihang University, Beijing 100191, China

^eDepartment of Physics, University of Stellenbosch, Stellenbosch, South Africa

Abstract

The low-lying collective states in Sn isotopes are studied by a five-dimensional collective Hamiltonian with parameters determined from the triaxial relativistic mean-field calculations using the PC-PK1 energy density functional. The systematics for both the excitation energies of 2_1^+ states and $B(E2; 0_1^+ \rightarrow 2_1^+)$ values are reproduced rather well, in particular, the enhanced $E2$ transitions in the neutron-deficient Sn isotopes with $N < 66$. We show that the gradual degeneracy of neutron levels $1g_{7/2}$ and $2d_{5/2}$ around the Fermi surface leads to the increase of level density and consequently the enhanced pairing correlations from $N = 66$ to 58. It provokes a large quadrupole shape fluctuation around the spherical shape, and leads to an enhanced collectivity in the isotopes around $N = 58$.

Keywords: covariant energy density functional, collective Hamiltonian, low-lying states, electromagnetic transition, Sn isotopes

PACS: 21.60.Jz, 21.60.Ev, 21.10.Re, 21.10.Tg

The evolution of shell structure and nuclear collectivity along either isotopic or isotonic chains, inferred from the systematics of the nuclear deformation energy surface [1], the nucleon separation energy [2, 3], the excitation energy of low-lying state and the electric quadrupole transition strength [4, 5], becomes of great interest in nuclear physics. In recent years, a number of experiments have measured the $B(E2; 0_1^+ \rightarrow 2_1^+)$ transition strengths in neutron-deficient Sn isotopes with $N < 66$ [6, 7, 8, 9, 10, 11, 12]. The deduced $B(E2)$ value increases when going from $N = 66$ to $N = 64$, and then remains roughly constant within the experimental uncertainties when decreasing the neutron number down to $N = 56$. This picture deviates from the parabolic trend, with a peak at mid-shell, predicted by the single j -shell seniority model [13]. Furthermore, the $B(E2)$ values deduced from the measurement of the lifetimes of the first excited 2^+ states in $^{112,114,116}\text{Sn}$ at the UNILAC accelerator of the Gesellschaft für Schwerionenforschung (GSI) are overall smaller than the previously reported values and present a shallow minimum at $N = 66$ [14]. These findings have generated a renewal interest in the study of low-lying states in Sn isotopes.

The theoretical description of the enhanced $B(E2; 0_1^+ \rightarrow 2_1^+)$ transition strength in the neutron-deficient Sn isotopes is not straightforward. Similarly as the seniority scheme, the seniority truncated large-scale shell model calculations predicted a nearly parabolic behavior of $B(E2)$ values with a maximum at $N = 66$ [6]. By using new interactions and including core polarization terms up to both the third order and $5\hbar\omega$ core excitations in the shell model calculations, the predicted $B(E2)$ values exhibit a shallow maximum around $N = 68 - 70$, but

are still far away from the experimental data [10]. Shell model calculations in the $sdgh$ major shell using CD-Bonn and Nijmegen1 two-body effective nucleon-nucleon (NN) interactions were also carried out for the mid-heavy even-even Sn isotopes in Refs. [15, 16]. An overall good agreement with the observed energy spectra of Sn isotopes is found. However, the $E2$ transitions are not presented. Recently, a quasiparticle-phonon model (QPM) was adopted to investigate the evolution of the 2_1^+ state in Sn isotopes [17]. The calculation reproduced the trend of the energies and, partly, the observed deviations of the $E2$ strengths from the parabolic behavior. It was shown that such an asymmetric trend was the consequence of several factors: single-particle energies, polarization of the $N = Z = 50$ core, interplay between pairing plus quadrupole, and quadrupole pairing interactions [17], all of which, however, are quite model-dependent.

In the framework of nuclear energy density functional theory or self-consistent Hartree-Fock-Bogoliubov (HFB) approach, due to the robust $Z = 50$ shell gap, the ground states of all the Sn isotopes are dominated by the spherical configuration. For the 2_1^+ states, which are expected to be a one-phonon state caused by surface vibration around the spherical shape, the theoretical studies are obviously beyond the mean-field approximation. For this purpose, one can either introduce random-phase approximation (RPA) or generator coordinate method (GCM), where the polarization of $N = Z = 50$ core in the shell model can be taken into account by particle-hole excitation in RPA or configuration mixing of different shapes in GCM. The implementations of the quasiparticle RPA on top of the nonrelativistic and relativistic mean-field calculations were carried out to

investigate the evolution of low-lying states along the Sn isotopic chain [18, 19, 20, 21]. In Refs. [19, 20], the systematics of $B(E2; 0_1^+ \rightarrow 2_1^+)$ values can be roughly reproduced. However, these studies were focused on the substantial rise of the $B(E2)$ values at neutron magic numbers 50 and 82, and did not provide any interpretation for the enhanced collectivity in the neutron-deficient Sn isotopes.

In recent years, the GCM has been introduced into the self-consistent mean-field approaches by combing with projection techniques in the modern energy density functional calculations [22, 23, 24, 25, 26, 27, 28, 29]. The dynamic correlation effects related to the symmetry restoration and quadrupole fluctuation (along both β and γ directions) around the mean-field minimum could be taken into account. These methods restricted to axial case have been applied to study the low-lying collective excitation spectra of the neutron-deficient Pb isotopes [30, 31]. However, the application of these methods with triaxial degree-of-freedom for systematic study is still much time-consuming. Up to now, such kind of study is mostly restricted to light nuclei [32, 33] and some specific medium heavy nuclei [34, 35]. As the Gaussian overlap approximation of GCM, collective Hamiltonian with parameters determined by self-consistent mean-field calculations is much simple in numerical calculations, and has achieved great success in description of nuclear low-lying states for deformed and transitional nuclei [36, 37, 38, 39, 40, 41, 42, 43, 44, 45, 46].

In the past decades, the covariant density functional theory (CDFT) has achieved great success in the description of nuclear structure over almost the whole nuclide chart, from light systems to superheavy nuclei, and from the valley of β stability to the particle drip lines [47, 48, 49]. Recently, the implementation of the five-dimensional collective Hamiltonian (5DCH) based on the CDFT has been developed and given successful microscopic description for the nuclear shape transitions along both the isotopic and isotonic chains [5, 38, 40, 41, 42]. In this work, we are going to apply this approach to study the low-lying collective states, for the first time, in the semi-magic Sn isotopes. Our aim is to provide a microscopic mechanism for the enhanced $E2$ transitions in the neutron-deficient Sn isotopes.

In the calculation, we use a recent parameterized relativistic functional PC-PK1 [50] for the particle-hole channel, and a separable force [51, 52] for the particle-particle channel. The solution of the equation of motion for the nucleons is accomplished by an expansion of the Dirac spinors in a set of three-dimensional harmonic oscillator basis functions in Cartesian coordinates with 12 major shells. More details about the calculations can be found in Ref. [27, 38, 53]. The intrinsic triaxially deformed states are obtained as solutions of the self-consistent RMF+BCS equations constrained on the mass quadrupole moments related to the Bohr parameters (β, γ) varying $\beta \in [0.0, 0.6]$ and $\gamma \in [0^\circ, 60^\circ]$ with step size $\Delta\beta = 0.05$ and $\Delta\gamma = 10^\circ$.

The nuclear collective excitations associated with three-dimensional rotation and quadrupole fluctuations are described with a five-dimensional collective Hamiltonian (5DCH). The dynamics of the 5DCH is governed by the seven functions of the

intrinsic deformations β and γ : the collective potential V_{coll} , the three mass parameters: $B_{\beta\beta}, B_{\beta\gamma}, B_{\gamma\gamma}$, and the three moments of inertia \mathcal{I}_k . These functions are determined using cranking approximation formula based on the intrinsic triaxially deformed states. The diagonalization of the Hamiltonian yields the excitation energies and collective wave functions that are used to calculate observables [38].

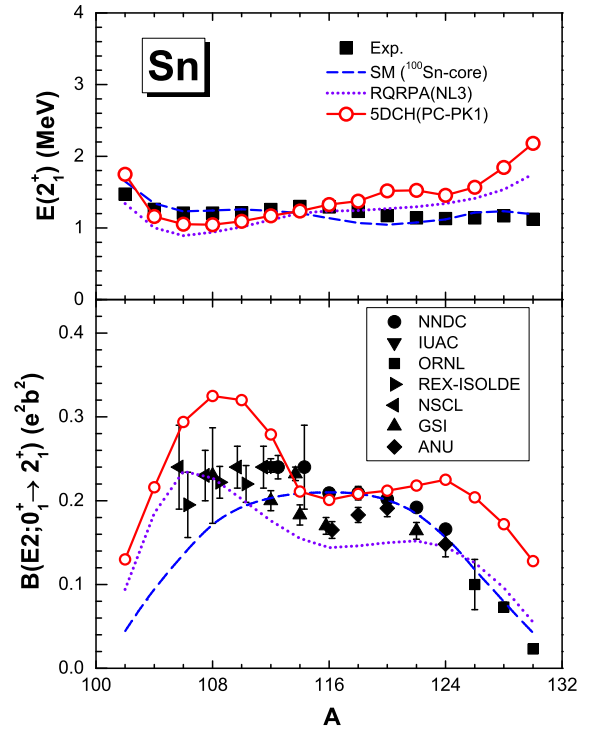


Figure 1: (Color online) Calculated $E(2_1^+)$ (upper panel) and $B(E2; 0_1^+ \rightarrow 2_1^+)$ (lower panel) in Sn isotopic chain by the shell model with ^{100}Sn core (dashed line), RQRPA (dotted line), and 5DCH based on PC-PK1 density functional (solid line with open circles), in comparison with the data (solid symbols). In the lower panel, the measured $B(E2; 0_1^+ \rightarrow 2_1^+)$ values from different experiments are indicated with different symbols.

The upper panel of Fig. 1 displays the excitation energies of 2_1^+ states for Sn isotopes from our 5DCH calculations, in comparison with those by the shell model with ^{100}Sn core and RQRPA calculations, as well as the data. The trend of the excitation energies of 2_1^+ states along the isotopic chain is reproduced quite well by the three models. It is notable that our 5DCH calculations give quite similar results as those by the RQRPA calculations, although the realization of these two models for excitation states are quite different. Compared with the shell model calculation, the discrepancy between our 5DCH result and the data is relatively larger for $^{120-130}\text{Sn}$, from ~ 200 keV to ~ 1 MeV. However, it is worthwhile to note that the 5DCH is fully self-consistent and without any free parameter. In addition, we find that, beside 2_1^+ state, the excitation energies of other low-lying states for $^{108-116}\text{Sn}$ are described as well as that by the recent shell model calculations [15, 16]. Taking ^{116}Sn as an example one finds that the *rms* deviation for seven low-lying excitation states (the first two 0^+ , three 2^+ , and two 4^+) is: $\sigma = 0.279$ MeV for the 5DCH, which is in compari-

son with the corresponding value 0.429 MeV obtained by using Nijmegen1 effective interaction in Ref. [15], and 0.137 MeV in the calculation of Ref. [16].

In the lower panel of Fig. 1, we present the $B(E2; 0_1^+ \rightarrow 2_1^+)$ values from 5DCH calculations, in comparison with the results by shell model and RQRPA, as well as the recently measured data. It is shown that both the 5DCH and RQRPA calculations reproduce rather well the systematics of $B(E2; 0_1^+ \rightarrow 2_1^+)$ values in the whole isotopic chain, in particular the increase of $E2$ strength from ^{116}Sn down to ^{108}Sn , which cannot be described by the shell model. Quantitatively, the RQRPA slightly underestimates those $E2$ strengths around ^{116}Sn . While the 5DCH overestimates the $E2$ strength $\sim 0.1 e^2 b^2$ when approaching to the neutron shell closure, where the low-lying states are mainly caused by the excitation of few quasiparticles. Concerning our interest and the power of our model, in the following we will mainly focus on the isotopes around middle shell, where the excitation is dominated by the collective vibration and enhanced $E2$ transition is observed.

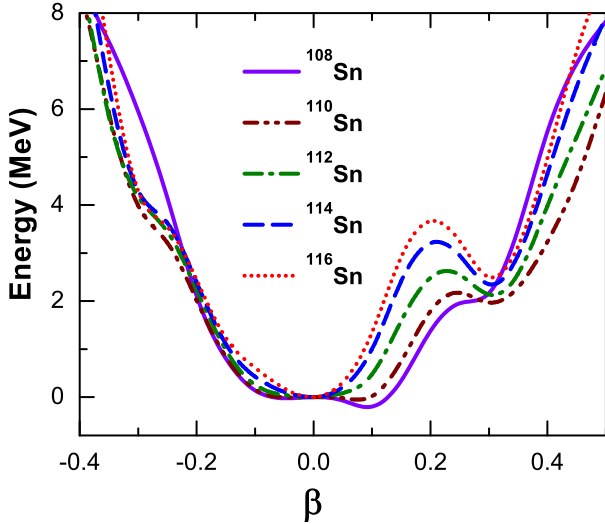


Figure 2: (Color online) Self-consistent RMF+BCS binding energy curves for the even-even $^{108-116}\text{Sn}$ isotopes as functions of the axial deformation parameter β . Energies are normalized with respect to the binding energy of the corresponding spherical state.

To understand the enhanced $E2$ transitions around $N = 108$, we plot the deformation energy curves of the even-even $^{108-116}\text{Sn}$ isotopes as functions of the axial deformation parameter β in Fig. 2. Due to the robust $Z = 50$ proton shell, all the Sn isotopes are spherical or near spherical. Around the neutron mid-shell $N = 66$, an excited prolate minimum with $\beta \sim 0.3$ shows up. As the decrease of the neutron number from $N = 66$ down to $N = 58$, the energy curve around spherical shape becomes softer gradually. In particular, for ^{108}Sn , a weakly prolate deformed global minimum with $\beta \sim 0.1$ is observed. In other words, the dynamic effect of quadrupole deformation fluctuations is enlarging the nuclear collectivity gradually when decreasing neutron number from $N = 66$ down to $N = 58$.

The upper panel of Fig. 3 displays the curvatures of the deformation energy curves around the spherical shape as a function

of neutron number. A rapid drop of the curvature in Sn isotopes with $A < 116$ is found, which is responsible for the increased $B(E2)$ value shown in Fig. 1. To understand this change in the topograph of deformation energy curves, we plot the average neutron pairing gaps, weighted by uv coefficient as Ref. [54], at spherical states in the lower panel of Fig. 3. For comparison, the odd-even mass differences of experimental data by the five-point formula are also plotted. It is shown that the rapid drop of the curvature when decreasing neutron number from $N = 66$ is closely correlated to the neutron pairing gaps. Similar evolution trend is shown in the odd-even mass differences. It indicates that the strong pairings soften the energy curve around spherical shape, which leads to the enhanced collectivity in Sn isotopes around $N = 58$.

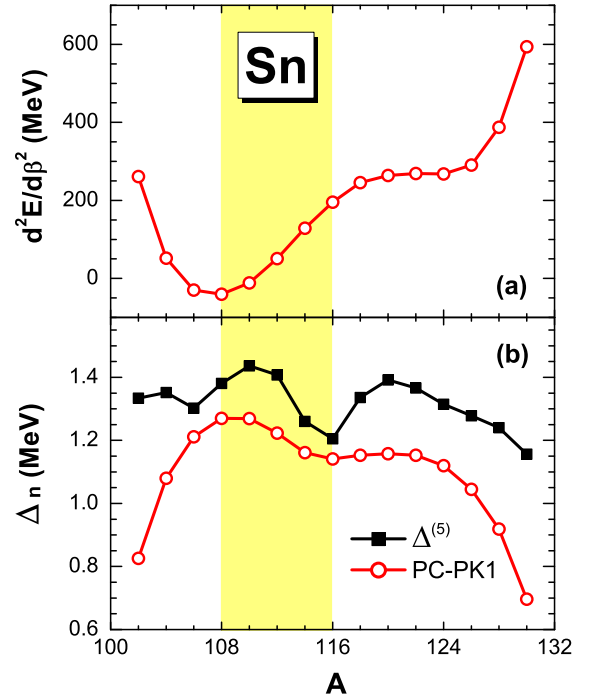


Figure 3: (Color online) The predicted curvature of the PEC (panel a) and average neutron pairing gaps (panel b) at spherical point in Sn isotopic chain calculated by PC-PK1 density functional. For comparison, the odd-even mass differences (denoted by solid squares) extracted by the five-point formula are also plotted in panel b.

Figure 4 displays the neutron single-particle energies at spherical shape along Sn isotopic chain. The balls indicate the position of Fermi surface. It is seen that the levels $1g_{7/2}$ and $2d_{5/2}$ move closer as the neutron number decreases from $N = 82$ to $N = 50$ shell. Meanwhile, the Fermi surface comes toward to these two levels for the isotopes with $A < 116$. This leads to the increasing level density around Fermi surface and consequently enhanced pairing correlations. Moreover, it is found that the Fermi surface crosses the $3s_{1/2}$ orbit in between $N = 64$ and $N = 70$. The considerable occupation probability of $3s_{1/2}$ orbit hinders the collectivity of these nuclei. Meanwhile, the obstructive effect is further enhanced by the low density of single-particle states around the Fermi surface, which reduces the pair correlations (c.f. in Fig. 3). It provides a qual-

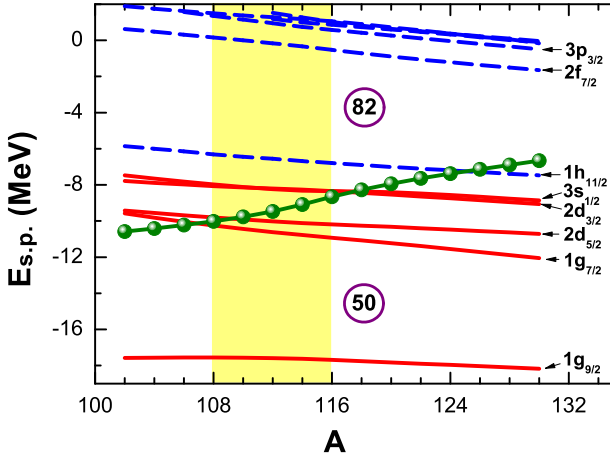


Figure 4: (Color online) Evolution of neutron single-particle levels at spherical point for Sn isotopic chain. The balls indicate the position of Fermi surface.

itative interpretation of the dip of $E2$ transition at ^{116}Sn , which is consistent with that given in Ref. [14].

In summary, the low-lying collective states in Sn isotopes from $N = 50$ to $N = 82$ have been studied by solving a five-dimensional collective Hamiltonian with parameters determined from the triaxial relativistic mean-field calculations. The calculations reproduce the systematics of both excitation energies for 2_1^+ states and $B(E2; 0_1^+ \rightarrow 2_1^+)$ rather well. In particular, the enhancement of $E2$ transitions from $N = 66$ to $N = 58$ has been found to be the consequence of increasing quadrupole shape fluctuation around spherical shape, induced by the strengthening neutron pairing correlations. This conclusion is consistent with that by the shell models, but in the language of mean-field approach. Furthermore, it is found the gradual degeneracy of levels $1g_{7/2}$ and $2d_{5/2}$ around the Fermi surface that leads to the increase of level density and consequently the enhanced pairing correlations. Moreover, it has shown that the Fermi surface crosses the $3s_{1/2}$ orbit in between $N = 64$ and $N = 70$, where the low level density and considerable occupation probability of $3s_{1/2}$ orbit hinder the nuclear collectivity and give rise to valley-like of the $E2$ transition as a function of neutron number.

Acknowledgments

This work was supported in part by the Major State 973 Program 2013CB834400, the NSFC under Grant Nos. 10975008, 10947013, 11175002, 11105110, and 11105111, the Research Fund for the Doctoral Program of Higher Education under Grant No. 20110001110087, the Southwest University Initial Research Foundation Grant to Doctor (Nos. SWU110039, SWU109011), the Fundamental Research Funds for the Central Universities (XDJK2010B007 and DJK2011B002).

References

[1] J. Meng, W. Zhang, S. G. Zhou, H. Toki and L. S. Geng, Eur. Phys. J. A 25 (2005) 23.

[2] R. F. Casten and E. A. McCutchan, J. Phys. G 34 (2007) R285.
[3] H. Z. Liang, P. W. Zhao, L. L. Li, and J. Meng, Phys. Rev. C 83 (2011) 011302(R).
[4] P. Cejnar, J. Jolie, and R. F. Casten, Rev. Mod. Phys. 82 (2010) 2155.
[5] Z. P. Li, T. Nikšić, D. Vretenar, J. Meng, G. A. Lalazissis, and P. Ring, Phys. Rev. C 79 (2009) 054301.
[6] A. Banu et al., Phys. Rev. C 72 (2005) 061305(R).
[7] J. Cederkäll et al., Phys. Rev. Lett. 98 (2007) 172501.
[8] C. Vaman et al., Phys. Rev. Lett. 99 (2007) 162501.
[9] J.N. Orce et al., Phys. Rev. C 76 (2007) 021302(R).
[10] A. Ekström et al., Phys. Rev. Lett. 101 (2008) 012502.
[11] P. Doornenbal et al., Phys. Rev. C 78 (2008) 031303(R).
[12] R. Kumar et al., Phys. Rev. C 81 (2010) 024306.
[13] I. Talmi, *Simple Models of Complex Nuclei*, Harwood Academic Publishers, 1993.
[14] A. Jungclaus et al., Phys. Lett. **B695** (2011) 110.
[15] E. Dikmen, O. Öztürk, and M. Vallieres, J. Phys. G 36 (2009) 045102.
[16] P. Guazzoni et al., Phys. Rev. C 83 (2011) 044614.
[17] N. Lo Iudice, Ch. Stoyanov, and D. Tarpanov, Phys. Rev. C 84 (2011) 044314.
[18] J. Terasaki, Nucl. Phys. **A746** (2004) 583c.
[19] A. Ansari, Phys. Lett. **B623** (2005) 37.
[20] A. Ansari, P. Ring, Phys. Rev. C 74 (2006) 054313.
[21] Y. Tian, Z. Y. Ma, and P. Ring, Phys. Rev. C 79 (2009) 064301.
[22] A. Valor, P. H. Heenen, and P. Bonche, Nucl. Phys. **A671** (2000) 145.
[23] R. Rodríguez-Guzmán, J. L. Egido, and L. M. Robledo, Nucl. Phys. **A709** (2002) 201.
[24] T. Nikšić, D. Vretenar, and P. Ring, Phys. Rev. C 73 (2006) 034308; C 74 (2006) 064309.
[25] M. Bender and P.-H. Heenen, Phys. Rev. C 78 (2008) 024309.
[26] J. M. Yao, J. Meng, D. Pena Arteaga, and P. Ring, Chin. Phys. Lett. 25 (2008) 3609.
[27] J. M. Yao, J. Meng, P. Ring, and D. Pena Arteaga, Phys. Rev. C 79 (2009) 044312.
[28] J. M. Yao, J. Meng, P. Ring and D. Vretenar, Phys. Rev. C 81 (2010) 044311.
[29] T. R. Rodríguez and J. L. Egido, Phys. Rev. C 81 (2010) 064323.
[30] M. Bender, P. Bonche, T. Duguet, and P.-H. Heenen, Phys. Rev. C 69, 064303 (2004).
[31] R. R. Rodríguez-Guzman, J. L. Egido and L. M. Robledo, Phys. Rev. C 69, 054319 (2004).
[32] J. M. Yao, H. Mei, H. Chen, J. Meng, P. Ring, and D. Vretenar, Phys. Rev. C 83 (2011) 014308.
[33] J. M. Yao, J. Meng, P. Ring, Z. X. Li, Z. P. Li, and K. Hagino, Phys. Rev. C 84 (2011) 024306.
[34] T. R. Rodríguez and J. L. Egido, Phys. Rev. C 84 (2011) 051307
[35] T. R. Rodríguez and J. L. Egido, Phys. Lett. **B705** (2011) 255.
[36] J. Libert, M. Girod, and J.-P. Delaroche, Phys. Rev. C 60 (1999) 054301.
[37] L. Próchniak, P. Quentin, D. Samsoen, and J. Libert, Nucl. Phys. **A730** (2004) 59.
[38] T. Nikšić, Z. P. Li, D. Vretenar, L. Próchniak, J. Meng, and P. Ring, Phys. Rev. C 79 (2009) 034303.
[39] N. Hinohara, K. Sato, T. Nakatsukasa, M. Matsuo, and K. Matsuyanagi, Phys. Rev. C 82 (2010) 064313.
[40] Z. P. Li, T. Nikšić, D. Vretenar, and J. Meng, Phys. Rev. C 80 (2009) 061301(R).
[41] Z. P. Li, T. Nikšić, D. Vretenar, and J. Meng, Phys. Rev. C 81 (2010) 034316.
[42] Z. P. Li, J. M. Yao, D. Vretenar, Nikšić, H. Chen, and J. Meng, Phys. Rev. C 84 (2011) 054304.
[43] T. Nikšić, D. Vretenar and P. Ring, Prog. Part. Nucl. Phys. 66 (2011) 519.
[44] J. M. Yao, Z. P. Li, K. Hagino, M.Thi Win, Y. Zhang, J. Meng, Nucl. Phys. **A868** (2011) 12.
[45] H. Mei, J. Xiang, J. M. Yao, Z. P. Li, and J. Meng, Phys. Rev. C 85 (2012) 034321.
[46] J. -P. Delaroche, M. Girod, J. Libert, H. Goutte, S. Hilaire, S. Péru, N. Pillet, and G. F. Bertsch, Phys. Rev. C 81 (2010) 014303.
[47] M. Bender, P.-H. Heenen, and P.-G. Reinhard, Rev. Mod. Phys. 75 (2003) 121.
[48] D. Vretenar, A. V. Afanasjev, G. A. Lalazissis, and P. Ring, Phys. Rep. 409 (2005) 101.

- [49] J. Meng, H. Toki, S. G. Zhou, S. Q. Zhang, W. H. Long, and L. S. Geng, *Prog. Part. Nucl. Phys.* **57** (2006) 470.
- [50] P. W. Zhao, Z. P. Li, J. M. Yao, and J. Meng, *Phys. Rev. C* **82** (2010) 054319.
- [51] Y. Tian, Z. Y. Ma, and P. Ring, *Phys. Lett.* **B676** (2009) 44.
- [52] T. Nikšić, P. Ring, D. Vretenar, Y. Tian, and Z. Y. Ma, *Phys. Rev. C* **81** (2010) 054318.
- [53] J. Xiang, Z.P. Li, Z.X. Li, J.M. Yao, J. Meng, *Nucl. Phys.* **A873** (2012) 1.
- [54] M. Bender, K. Rutz, P.-G. Reinhard, and J. A. Maruhn, *Eur. Phys. J. A* **8** (2000) 59.